Compositionally matched Nitrogen-doped $Ge_2Sb_2Te_5/Ge_2Sb_2Te_5$ Superlattice-like Structures for Phase Change Random Access Memory

Chun Chia Tan[1,2], Luping Shi[3], Rong Zhao[4a)], Qiang Guo[5], Yi Li[6], Yi Yang[1], Tow Chong Chong[4], Jonathan A. Malen[7], Wee-Liat Ong[7], Tuviah. E. Schlesinger[2], James A. Bain[2b)]

[1]Data Storage Institute, A*STAR (Agency for Science, Technology and Research), DSI Building, 5 Engineering Drive 1, Singapore 117608

[2]Department of Electrical and Computer Engineering, Carnegie Mellon University, 5000 Forbes Avenue, Pittsburgh, PA 15213-3890

[3]Optical Memory National Engineering Research Center, Department of Precision Instrument, Tsinghua University, Beijing 100084, China

[4]Singapore University of Technology & Design, 20 Dover Drive Singapore 138682

[5]State Key Laboratory of Metal Matrix Composites, Shanghai Jiao Tong University, 800 Dongchuan Road, Shanghai, 200240, People's Republic of China

[6]Department of Material Science and Engineering, National University of Singapore, 7 Engineering Drive 1, Singapore 117576

[7]Department of Mechanical Engineering, Carnegie Mellon University, Pittsburgh, 5000 Forbes Avenue, Pittsburgh, PA 15213-3890

[a)] Author to whom correspondence should be address: Zhao Rong, Electronic Mail: zhao_rong@sutd.edu.sg
[b)] Author to whom correspondence should be address: James A. Bain, Electronic Mail: jbain@ece.cmu.edu

Abstract:

A compositionally matched superlattice-like (SLL) structure comprised of $Ge_2Sb_2Te_5$ (GST) and nitrogen-doped GST (N-GST) was developed to achieve both low current and high endurance Phase Change Random Access Memory (PCRAM). N-GST/GST SLL PCRAM devices demonstrated ~37% current reduction compared to single layered GST PCRAM and significantly higher write/erase endurances of $\sim 10^8$ compared to $\sim 10^6$ for $GeTe/Sb_2Te_3$ SLL devices. The improvements in endurance are attributed to the compositionally matched N-GST/GST material combination that lowers the diffusion gradient between the layers and the lower crystallization-induced stress in the SLL as revealed by micro-cantilever stress measurements.

Phase Change Random Access Memory (PCRAM) is a promising next generation non-volatile memory technology due to its excellent data retention, high endurance and good scalability.[1] $Ge_2Sb_2Te_5$ (GST) is a phase change material often used in prototype PCRAM devices because it offers both speed and stability.[2] Nevertheless, the relatively high programming current required to RESET GST-based devices from the low resistance state to the high resistance state will limit the ultimate achievable density.[3] This has led to the development of various approaches to reduce this RESET programming current.

Apart from using novel device structures[4,5] and materials[6], superlattice-like (SLL) or multi-layered structures[7,8] have also proven to be a very effective concept to lower the programming current. Chong *et al*[8] pioneered the development of the SLL concept where a SLL structure composed of nano-scale layers of GeTe and Sb_2Te_3 alternatingly stacked was utilized in PCRAM. These SLL PCRAM cells demonstrated lower RESET currents with faster write/erase speeds compared to conventional GST PCRAM cells and the improvements have fueled a growing interest in understanding and improving the SLL structure.[9,10] Despite SLL structures displaying reduced currents, SLL structures are expected to have poorer endurance/reliability since phase change materials with different material properties (such as stoichiometric composition and lattice constants) are used to create the SLL. SLL layers with different stoichiometry could drive inter-layer diffusion while the different lattice constants will increase crystallization-induced stress thus impacting the reliability of SLL PCRAMs.[11] Furthermore, the nanometer thickness phase change materials within the SLL structures will exacerbate the stress as the crystallization-induced stress increases with the decrease in layer thickness.[12] While reliability is important for the SLL to switch repeatedly, the impact of stress on cell endurance/reliability in SLL structures has not been well studied.

In this letter, we propose and implement a reduced stress SLL system with a compositionally matched material combination to concurrently improve SLL PCRAM endurance and reduce the RESET current. This SLL structure consists of layers of GST and nitrogen-doped GST (N-GST) that have similar compositions except for the addition of nitrogen in the N-GST. Various configurations of the N-GST/GST SLL structure are implemented in PCRAM devices to examine switching performance. Following that, reliability and endurance of the N-GST/GST SLL structures are reported. To understand the impact of having composition matching in SLL structures, the evolution of the crystallization-induced stress with temperature in SLL structures was also analyzed.

The choice of materials is important in the construction of the SLL PCRAM. GST is a common phase change material that has a metastable NaCl, face-centered cubic (FCC)[2] polycrystalline structure and its properties can be enhanced significantly through doping by various elements.[13] Nitrogen is commonly incorporated in GST (as N-GST) with an optimal concentration to improve the endurance.[14] It was also found that nitrogen doping of GST prevents the electro-migration of the N-GST constituent elements during electrical stressing.[15] The advantage of N-GST and GST pairing is evident since the crystal structure for N-GST with low nitrogen concentrations remains nearly the same as the undoped GST FCC structure with some strained bonds that slightly increase the lattice constant[16]. At the same time the similar composition reduces the drive for intermixing of the layers. The choice of nitrogen concentration is critical in the design of the N-GST/GST SLL. If N-GST is doped heavily with nitrogen (>6.2 at. %)[14], it will crystallize to form a hexagonal structure. X-ray diffraction spectra of GST and N-GST(4 at. %) shown in Tan *et al*[17] indicate that both films have a FCC rock salt structure after annealing at 300 °C. Using the (200) peak, the stressed lattice constant of GST and N-GST films

were calculated to be ~0.6056 nm and ~0.6096 nm respectively. The lattice constant increase due to nitrogen doping translates to a small difference of ~0.67 %. In view of these considerations, N-GST (4 at. %) is chosen to be paired with GST to create the nearly lattice matched N-GST/GST SLL structure. For the rest of the letter, all the N-GST films discussed have a nitrogen doping concentration of ~4 at. %.

To investigate the performance of the N-GST/GST SLL structures, PCRAM devices with single layer GST, single layer N-GST and SLL N-GST/GST structures were fabricated. All the devices had the same via structure and the films were deposited using physical vapor deposition (PVD). Flowing a controlled mixture of argon (15 sccm) and nitrogen gas (3 sccm) during the PVD from a composite GST target resulted in N-GST films (sputter pressure: ~3.1×10^{-3} Torr). The N-GST/GST SLL films were deposited by alternating deposition of N-GST and GST films. TiW films were used as the top and bottom electrodes. The critical contact area between the phase change materials and the electrode for all devices was defined by patterning SiO_2 to create a via with a diameter of ~1 μm. A cross-sectional schematic of the single constituent PCRAM devices and SLL devices with N-GST/GST SLL structures is shown in Fig. 1(a) and (b) respectively. In what follows, the number of described SLL layers is the total number of N-GST and GST layers within the device. The total thickness of PCRAM switching layers within the device (bulk N-GST, bulk GST and SLL structures) is ~50 nm. As the number of layers within the SLL is increased, the thickness of the layers is reduced to keep the total thickness at 50 nm.

The plots of resistance vs RESET current (30 ns pulse width) for GST, N-GST and 12-layered N-GST /GST SLL devices (each layer with thickness of ~4.2 nm) are displayed in Fig. 2(a). It is observed that the RESET current of the 12-layered SLL device is ~37 % less than that of the single-layered GST device. This is close to the RESET current reduction achieved by

the $GeTe/Sb_2Te_3$ SLL devices reported previously.[8] The device performance with different N-GST/GST SLL configurations was systematically examined by changing the number of layers while keeping the total thickness constant at ~50 nm. The RESET current for different N-GST/GST SLL structures (indicated by number of layers) is plotted in Fig. 2(b). It is observed that the current gradually decreases as the number of layers increases from 4 to 12 layers. As the number of layers is further increased to 16, the current shows a large increase. The 12-layered SLL device was found to have the lowest RESET current. Several explanations such as decreased thermal conductivity due to layering[10] and reduction of entropy losses[9] have been proposed for the current reduction exhibited in multi-layered PCRAM devices. This debate is ongoing and is not the focus of this work. We believe that the reason for the increase of the RESET current at 16 layers is due to the fact that the layers are very thin. It was found that ultrathin GST and N-GST films[18] directly crystallize into the HCP crystal structure which is deemed to be more stable and thus requires more RESET current to carry out the melt-quench transition.[14]

To analyze the effect of repeated switching on the layered SLL structures, the cross-section of a N-GST/GST SLL device which was subjected to 10^4 switching cycles between the amorphous and crystalline phase was observed using high resolution transmission electron microscopy (HR-TEM) as shown in Fig. 3(a). Despite the numerous switching cycles, the SLL still maintained its distinct GST and N-GST layers, indicating that any intermixing during switching is insufficient to homogenize the sample. The black regions above and below the SLL are the TiW electrodes. Diffusion length calculations based on reported endurance switching of PCRAM devices[5,19,20] indicate that Ge, Sb and Te elements require ~1.26×10^4 cycles before significant intermixing of atoms between the layers and this is consistent with our TEM image. It

is interesting to note that diffusion constants of GST derived from molecular simulations[21] range from 3.78×10^{-5} to 4.67×10^{-5} cm^2/s and this may result in a diffusion length of ~20 nm after a 20 ns pulse. The large diffusion lengths might not allow GeSbTe based devices to switch 10^9 to 10^{11} times and so the diffusion constants were estimated from actual endurance data[5,19,20] (~10^{-15} cm^2/s). The reason for the large difference in magnitude may be due to the different conditions considered in the two cases. We note that the molecular simulations were conducted for time scales of ps while the diffusion constants we derived in the endurance experiments were carried out over ns. The second reason is that in pulse endurance experiments, the period above melting point is shorter than the pulse width applied. Another reason is that the molecular simulation is carried out in an open system, however the diffusion in a device happens in an embedded environment.

The endurance and reliability of the N-GST/GST SLL and $GeTe/Sb_2Te_3$ SLLs fabricated using the same methods were investigated by repeatedly switching the cells between their amorphous and crystalline state using fixed RESET and SET voltage pulses. The normalized crystalline and amorphous resistance of the SLL devices were recorded at intervals and plotted in Fig. 3(c). It can be seen that the N-GST/GST SLL device could be switched reversibly ~10^8 times with the amorphous to crystalline resistance maintaining more than one order of magnitude difference without any write errors. Similar to the 12-layer device, all the N-GST/GST devices with other SLL configurations were capable of switching more than 10^8 times. It was found that after 10^9 times of switching events, the layered structure was no longer intact as observed in cross-section of a failed SLL PCRAM device (Fig. 3(b)). Interdiffusion of the layers due to repeated switching could cause the migration of Ge, Sb and Te atoms[15] to form a composition significantly different from GST and this possibly is one of the causes of SLL PCRAM failure.

Despite this, 10^8 times of endurance is significantly higher than a $GeTe/Sb_2Te_3$ SLL device fabricated using similar methods which was only capable of switching reversibly ~10^6 times before failing (Fig. 3(c)). A previously reported $GeTe/Sb_2Te_3$ SLL structure with similar 1 μm feature size had an endurance of ~10^7 cycles.[8] One hypothesis for the improved endurance of the N-GST/GST SLL device is that the constituent material layers are of similar composition which reduces the driving force for interdiffusion. We speculate that a second reason for the one to two order-of-magnitude improvement in cyclability endurance is due to a reduction in the crystallization-induced stress gradient.[22]

The impact of composition matching to reduce stress in layered structures for high endurance was examined by studying the crystallization-induced stress of the N-GST/GST SLL and $GeTe/Sb_2Te_3$ SLL using a micro-cantilever method proposed by Guo *et al*[12]. These SLL structures were deposited on top of low stress SiN micro-cantilevers as shown in Fig. 4(a). In their as-deposited state, the SLL structures were amorphous and the cantilevers displayed less than 1 μm deflection (within the measurement error of +/- 1 μm) indicating that the net residual stress in the film as a result of the deposition was negligible. These cantilevers were then subjected to thermal annealing at various temperatures ranging from 120 °C to 260 °C. The cantilever deflections were measured after each annealing temperature and their corresponding stress was calculated using the revised Stoney equation (derived in Chapter 2 of ref 20) for thin substrate conditions[23] and using GST's biaxial modulus of 45.2 GPa.[24] It is important to note that all measurements were made at room temperature after the films were exposed to the temperature indicated on the x-axis for 120 s. Thus, thermally induced elastic stresses that occur during heating and then are relieved upon cooling were not measured. Fig. 4(b) shows the average biaxial stress in the layered composite at various stages of crystallization for both SLL

structures. The crystallization of phase change materials results in a large volume/thickness change (~5.5 - 9 %) that causes crystallization-induced stress.[22] The crystallization event in each constituent layer of the two SLL structures can be deduced from the increases in stress levels in Fig. 4(b). For the GeTe/Sb_2Te_3 SLL, we interpret Fig. 4(b) to mean that from 120 - 160 °C, the Sb_2Te_3 layers crystallized completely and took up a FCC structure[25] while the GeTe layers remained amorphous. Following that, the film stress remained constant until 220 °C, after which the GeTe layers crystallized, leading to an additional decrease in volume and a further increase in film stress. For the N-GST/GST SLL, the GST layers crystallized over the temperatures from 120 to 220 °C, while the N-GST remained in the amorphous state. Above 240 °C, the N-GST layers crystallized as indicated by the rapid increase in the stress levels (Fig. 4(b)). This temperature range corresponds to the crystallization temperature of N-GST, which was found to be ~230 °C.

Assuming that the stress transitions in Fig. 4(b) (GST 120-220 °C, N-GST 240-260 °C, Sb_2Te_3 120-160 °C and GeTe 220-260 °C) are due to the additional force of each crystallizing layer while ignoring their partial crystallization and secondary transformations, the final stress states of the GST, N-GST, GeTe and Sb_2Te_3 layers can be extracted and are summarized in Table I. From Table I, it can be observed that the stress states of GST and N-GST differ by ~0.11 GPa while the stress states of GeTe and Sb_2Te_3 differ by ~0.24 GPa; more than twice the stress state difference of the N-GST/GST layers. As the N-GST and GST layers show a small difference in stress states, it is expected that their volume change difference is also small thus leading to a lower stress gradient within the SLL. Conversely, GeTe and Sb_2Te_3 layers exhibit significantly different stress levels because their volume change is significantly different and this results in higher stress gradients within the SLL as demonstrated by the overall stress

measurements in Fig. 4(b). Even though the average value of the stress states for each SLL is found to be quite similar in Table I, the stress gradients (indicated by the difference in the stress states of each layer) are significantly higher in the $GeTe/Sb_2Te_3$ SLL compared to the N-GST/GST SLL. We assert that these lower stress gradients (Table I) contribute to the higher switching endurances (Fig. 3(c)) observed in the N-GST/GST SLL compared to the $GeTe/Sb_2Te_3$ SLL. This is also consistent with the observation that the reduction of crystallization-induced stress is needed for enhanced device reliability.[11]

TABLE I: Summary of the stress states for each layer within the SLL

Layer	Final Stress State (GPa)	Error (GPa)	Stress Difference (GPa)	Average Stress (GPa)
Sb_2Te_3	0.19	0.014	0.24	0.31
GeTe	0.43	0.015		
N-GST	0.32	0.014	0.11	0.27
GST	0.21	0.015		

To conclude, a compositionally matched SLL structure based on N-GST and GST was developed to enable the realization of both low RESET current and high endurance in a PCRAM device. Electrical measurements indicate that the N-GST/GST SLL structures not only displayed significant reduction in the RESET current compared to the conventional GST device but also improved switching endurance compared to that reported for $GeTe/Sb_2Te_3$ SLL structures. The RESET current of the N-GST/GST SLL devices was found to vary with different SLL configurations, highlighting that the SLL properties can be optimized for low RESET current operations by changing the number of layers even while keeping the total thickness constant. Stress measurements suggest that compositional matching helps to reduce crystallization-induced stress gradients in SLL structures. The compositionally matched SLL material combination could be implemented in nano-sized PCRAM devices for reduced current and improved endurance. This work shows that the layered structures can play a significant role in the manipulation of phase change material properties and tailoring for improved device performance.

References:

[1] S. Lai, in *Tech. Dig. Inter. Electron Devices Meet.* (2003), pp. 10.1.1–10.1.4.

[2] N. Yamada, E. Ohno, K. Nishiuchi, N. Akahira, and M. Takao, J. Appl. Phys. **69**, 2849 (1991).

[3] Y.N. Hwang, S.H. Lee, S.J. Ahn, S.Y. Lee, K.C. Ryoo, H.S. Hong, H.C. Koo, F. Yeung, J.H. Oh, H.J. Kim, W.C. Jeong, J.H. Park, H. Horii, Y.H. Ha, J.H. Yi, G.H. Koh, G.T. Jeong, H.S. Jeong, and K. Kim, in *Tech. Dig. Inter. Electron Devices Meet.* (IEEE, 2003), pp. 37.1.1–37.1.4.

[4] D.H. Im, J.I. Lee, S.L. Cho, H.G. An, D.H. Kim, I.S. Kim, H. Park, D.H. Ahn, H. Horii, S.O. Park, U. Chung, and J.T. Moon, in *Tech. Dig. Inter. Electron Devices Meet.* (2008), pp. 1–4.

[5] J.Y. Wu, M. Breitwisch, S. Kim, T.H. Hsu, R. Cheek, P.Y. Du, J. Li, E.K. Lai, Y. Zhu, T.Y. Wang, H.Y. Cheng, A. Schrott, E.A. Joseph, R. Dasaka, S. Raoux, M.H. Lee, H.L. Lung, and C. Lam, in *Tech. Dig. Inter. Electron Devices Meet.* (2011), pp. 3.2.1–3.2.4.

[6] Y.C. Chen, C.T. Rettner, S. Raoux, G.W. Burr, S.H. Chen, R.M. Shelby, M. Salinga, W.P. Risk, T.D. Happ, G.M. McClelland, M. Breitwisch, A. Schrott, J.B. Philipp, M.H. Lee, R. Cheek, T. Nirschl, M. Lamorey, C.F. Chen, E. Joseph, S. Zaidi, B. Yee, H.L. Lung, R. Bergmann, and C. Lam, in *Tech. Dig. Inter. Electron Devices Meet.* 2006. 1-4

[7] H. Yang, T.C. Chong, R. Zhao, H.K. Lee, J. Li, K.G. Lim, and L. Shi, Appl. Phys. Lett. **94**, 203110 (2009).

[8] T.C. Chong, L.P. Shi, R. Zhao, P.K. Tan, J.M. Li, H.K. Lee, X.S. Miao, A.Y. Du, and C.H. Tung, Appl. Phys. Lett. **88**, 122114 (2006).

[9] R.E. Simpson, P. Fons, A. V. Kolobov, T. Fukaya, M. Krbal, T. Yagi, and J. Tominaga, Nature Nanotechnol. **6**, 501 (2011).

[10] H. Tong, X.S. Miao, X.M. Cheng, H. Wang, L. Zhang, J.J. Sun, F. Tong, and J.H. Wang, Appl. Phys. Lett. **98**, 101904 (2011).

[11] L. Krusin-Elbaum, C. Cabral, K.N. Chen, M. Copel, D.W. Abraham, K.B. Reuter, S.M. Rossnagel, J. Bruley, and V.R. Deline, Appl. Phys. Lett. **90**, 141902 (2007).

[12] Q. Guo, M. Li, Y. Li, L. Shi, T.C. Chong, J.A. Kalb, and C. V. Thompson, Appl. Phys. Lett. **93**, 221907 (2008).

[13] S. Privitera, E. Rimini, C. Bongiorno, A. Pirovano, and R. Bez, Nucl. Instr. and Meth. in Phys. Res. B **257**, 352 (2007).

[14] L.W.-W. Fang, R. Zhao, M. Li, K.-G. Lim, L. Shi, T.-C. Chong, and Y.-C. Yeo, J. Appl. Phys. **107**, 104506 (2010).

[15] T.-Y. Yang, J.-Y. Cho, and Y.-C. Joo, Electrochemical and Solid-State Letters **13**, H321 (2010).

[16] T.H. Jeong, M.R. Kim, H. Seo, J.W. Park, and C. Yeon, Jpn. J. Appl. Phys. Part 1 **39**, 2775 (2000).

[17] C.C. Tan, R. Zhao, L. Shi, T.C. Chong, J.A. Bain, T.E. Schlesinger, J.A. Malen, and W.L. Ong, in *Proc - Non-Volatile Memory Technol. Symp.* (IEEE, 2011), pp. 1–4.

[18] S. Raoux, J.L. Jordan-Sweet, and A.J. Kellock, J. Appl. Phys. **103**, 114310 (2008).

[19] I.S. Kim, S.L. Cho, D.H. Im, E.H. Cho, D.H. Kim, G.H. Oh, D.H. Ahn, S.O. Park, S.W. Nam, J.T. Moon, and C.H. Chung, in *Dig. Tech. Pap. - Symp. VLSI Technol* (IEEE, 2010), pp. 203 -204.

[20] D. Cai, H. Chen, Q. Wang, Y. Chen, Z. Song, G. Wu, and S. Feng, IEEE Electron Device Lett. **33**, 1270 (2012)

[21] J. Akola and R. Jones, Phys. Rev. B **76**, 235201 (2007).

[22] T.P.L. Pedersen, J. Kalb, W.K. Njoroge, D. Wamwangi, M. Wuttig, and F. Spaepen, Appl. Phys. Lett. **79**, 3597 (2001).

[23] L.B. Freund and S. Suresh, *Thin Film Materials: Stress, Defect Formation and Surface Evolution*, 1st ed. (Cambridge University Press, Cambridge, 2003).

[24] J. Kalb, F. Spaepen, T.P. Leervad Pedersen, and M. Wuttig, J. Appl. Phys. **94**, 4908 (2003).

[25] Y. Yin, H. Sone, and S. Hosaka, J. Appl. Phys. **102**, 064503 (2007).

Captions:

Figure 1:

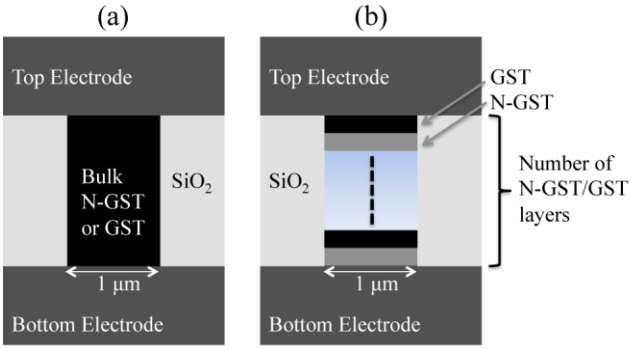

FIG. 1. Schematic cross-section of (a) N-GST and GST PCRAM and (b) N-GST/GST SLL PCRAM. Both devices have a 1 μm diameter contact area. The total thickness of the N-GST/GST SLL and the bulk phase change materials are kept at 50 nm. The number of layers of N-GST and GST in N-GST/GST SLL were varied and their thickness changed correspondingly to make up a total thickness of 50 nm.

Figure 2:

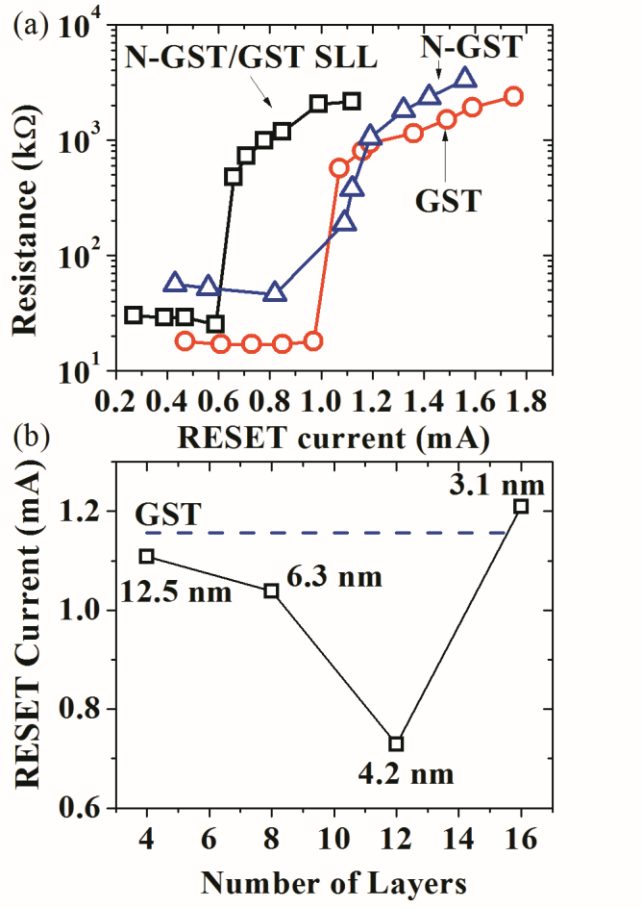

FIG. 2(a). RESET current curve of the single constituent and SLL PCRAM devices obtained using a current pulse width of 30 ns. (b) Variation of RESET current with different SLL configurations. The constituent layer thickness of the various SLL structures is displayed with their corresponding data points. The RESET current is found to decrease with increase in layer number, reaching a minimum RESET current at 12 layers. The RESET current increases when the layer number is increased from 12 to 16. The horizontal dashed line indicates the RESET current needed for GST PCRAM device.

Figure 3

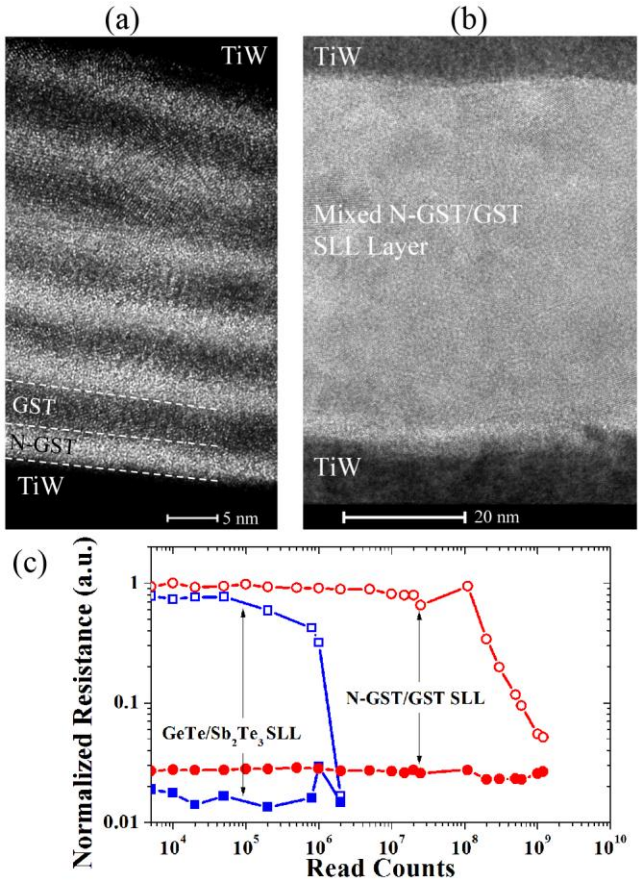

FIG. 3(a). High resolution-Transmission electron micrograph (HRTEM) image of the layered structure after cycling the device 10^4 times. The black regions on top and at the bottom of the SLL are the TiW electrodes. The GST and N-GST layers are as labeled. (b) Transmission electron Micrograph image of a failed N-GST/GST SLL device after 10^9 switching cycles. It was found that the layered structure mixed after 10^9 switching events. (c) Endurance of N-GST/GST SLL and GeTe/Sb_2Te_3 SLL PCRAM devices. The crystalline (full colored symbols) and amorphous (outlined symbols) resistances were normalized using the maximum resistance state recorded. The N-GST/GST SLL device was capable of having two distinct resistance states after cycling ~$1x10^8$ times while the GeTe/Sb_2Te_3 SLL device was only capable of switching ~10^6 times.

Figure 4:

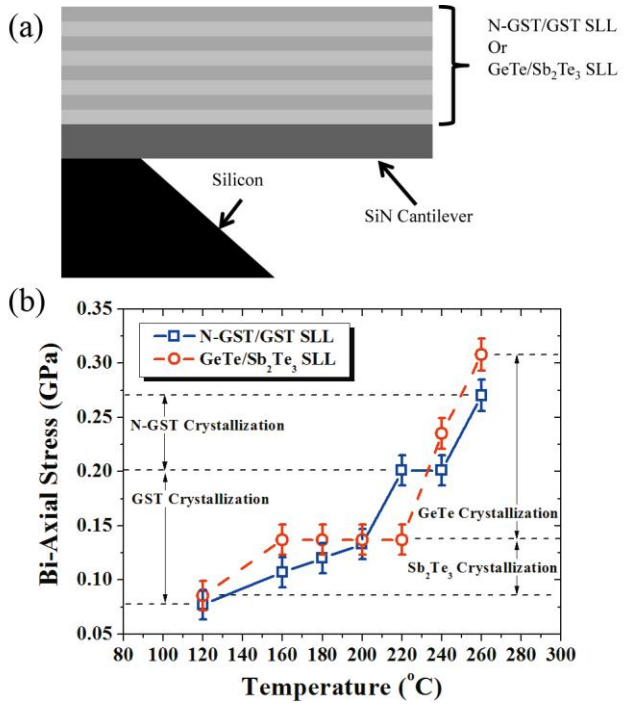

FIG. 4. (a) Cross-section of the SLL structure on the SiN cantilever and (b) Bi-axial stress of the two SLL structures annealed at different temperatures. The bi-axial stress was estimated using the bi-axial modulus of GST.

Table 1:

TABLE I: Summary of the stress states for each layer within the SLL

Layer	Final Stress State (GPa)	Error (GPa)	Stress Difference (GPa)	Average Stress (GPa)
Sb_2Te_3	0.19	0.014	0.24	0.31
GeTe	0.43	0.015		
N-GST	0.32	0.014	0.11	0.27
GST	0.21	0.015		